28th European Young Geotechnical Engineers Conference – EYGEC 2024
 ISBN xxx-xxx-xx-xxxx-x

Modeling and response of retaining wall subjected to strong ground motions

Maria K. Topalska[a]

[a]*Eng., University of Architecture Civil Engineering and Geodesy, Sofia, Bulgaria*

ABSTRACT

This research explores the seismic response of a flexible retaining wall, designed on a construction site in the city of Sofia, Bulgaria. Time-history analyses were carried out using the finite element modeling. The FEM models were created with Plaxis 2D software. The dynamic behaviour of structure and soil is investigated for a set of real accelerograms. A package of amplitude and integral parameters of the earthquakes is analyzed for each accelerogram. Several strong ground motions whose characteristics are compatible with the geological conditions and frequency parameters of the soils on the construction site were selected. For the purpose of soil-structure interaction analysis the retaining structure is modeled as a linear elastic element. The specific non-linear behaviour of soils is modeled by using the complex constitutive laws HSsmall. According to the results from the performed solutions a comparative analysis is developed. The influence upon the seismic response of structure and soil of varying strong ground motion parameters is considered.

KEYWORDS

Embedded retaining wall; Seismic impact; Accelerogram; Time-history analysis

1. INTRODUCTION

The embedded retaining walls are a widespread method for an excavation support. Their relevance is mainly determined by the need of construction in densely build-up areas and the implementation of underground levels as part of residential and public buildings.

In most cases the decisive load combination for ultimate and serviceability limit state verification is the seismic one. In order to model the soil-retaining structure interaction for seismic impact, the classical approaches of pseudostatic methos are often applied. The pseudostatic methods suggest that the seismic earth pressure depends entirely on the peak ground acceleration *PGA* and remains constant through the time of loading. These methodologies do not explain the soil and structure`s real response during an earthquake event. For more accurate representation a nonlinear time-history analysis should be carried out. It gives the opportunity for more comprehensive description of the strong ground motion, material behaviour under cyclic loads and geometry of structure.

This study is aimed at investigation of the influence on the retaining structure`s stressed and deformed state of several peak and integral parameters of the strong ground motion. For the purpose of this a finite element modeling is conducted by the Plaxis 2D software. The seismic loading is presented by accelerograms. Six accelerograms are used with different ground motion characteristics. Before applying the impact in a FE model to a soil foundation with an adjacent retaining wall, the earthquake records are subjected to a deconvolution procedure. It consists of a process of evaluation of seismic motion at varying depths of a soil profile. The deconvolution is carried out by the ProShake 2.0 software. The retaining wall is modeled as linear elastic structure. To model the soil the HSsmall constitutive model is used. It successfully describes the nonlinear hysteretic behaviour of soil due to cyclic dynamic loading (such as the seismic one).

Studies on the values of the soil parameters according to the HSsmall model have been carried out in the sources (Kerenchev, 2015), (Kerenchev and Milev, 2019).

2. DESCRIPTION OF THE DESIGN STRUCTURE

For the purpose of the study an embedded retaining wall of the Soldier Pile Wall type is examined. The structure is designed to strengthen a deep excavation for the construction of a residential building in the city of Sofia. The geometry of the wall is shown on Figure 1. The vertical load-bearing elements are steel 2T profiles with an axial distance between them of 1,0m. The 2T profiles are 6,5m long. The embedded part is 1,5m long, so the exposed part is 5,0m long. The wall is single row supported by a brace at 45° related to the ground surface.

3. FINITE ELEMENT ANALYSES OF THE SOIL-RETAINING WALL INTERACTION

3.1. Two dimensional FE model

To investigate the soil-retaining wall interaction a plain strain numerical model is built using the Plaxis 2D software (Figure 2). The soil body is discretized by 15-node triangular elements with node displacements U_x and U_y in the xy plane. The wall is modeled by 5-node frame elements which work for bending moments, axial and shear forces. The soil-wall interaction is modeled by interface elements. Along the border of the assumed soil body a damper boundary condition is associated for the purpose of absorbing seismic energy and thus simulating an infinite soil space.
The mesh generation in Plaxis 2D is automatic but it can be controlled and changed. When it comes to dynamic analysis the size of the finite element has to be synchronized with the frequency content of the input motion and the shear wave velocity. According to (Kuhlmeyer and Lysmer, 1973) the average element size *AES* is expressed by Equation 1.

$$AES \le \frac{V_{s,\min}}{8 f_{\max}}, \tag{1}$$

where: $V_{s,min}$ – the lowest shear wave velocity [m/s^2], f_{max} – the maximum frequency of the input wave [Hz].

Five stages of excavation works are simulated. Calculations and obtained results refer to 1,0 m of the structure.

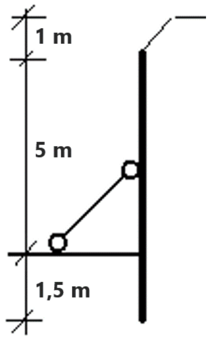

Figure 1. Structure`s cross section

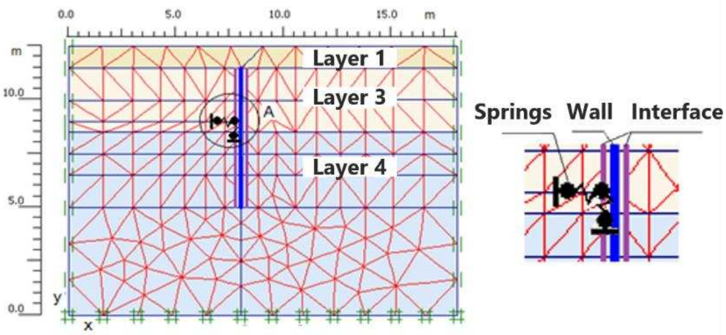

Figure 2. Finite element plane strain model

3.2. Geotechnical materials

The behaviour of dispersed soils under cyclic dynamic impact is described by the Hardening Soil Small (HSsmall) model. According to this model the soil is represented as nonlinear elastoplastic material. It takes into account for the stiffness degradation of the soil due to cyclic dynamic impact. The decreased stiffness is expressed by the shear modulus reduction G/G_{max}, depending on the shear strain γ. The adopted diagram for volumetric strains ε is shown in (Schanz et al., 1999). A typical diagram for the shear modulus reduction curve can be seen in (Kramer, 1996). The HSsmall model uses the Mohr-Column failure criteria and a set of parameters for the soil layers, which are shown in Table 1.

Table 1, Conventional soil characteristics and parameters of the HSsmall model

Parameter	Symbol	Measure	Layer 1	Layer 3	Layer 4
Bulk density	γ_n	kN/m^3	18,0	20,0	18,5
Cohesion	C	kPa	24,0	31,8	26,0
Angle of friction	φ	°	18,0	34,0	19,0
Reference stress for stiffness	p_{ref}	kPa	100	100	100
Tangent stiffness for primary oedometer loading	$E_{oed,ref}$	kPa	12 000	26 000	20 000
Secant stiffness in the standard drained triaxial test	$E_{50,ref}$	kPa	12 000	26 000	20 000
Unloading/Reloading stiffness	$E_{ur,ref}$	kPa	36 000	80000	60 000
Initial shear modulus	$G_{0,ref}$	kPa	80 000	150 000	120 000
Poisson's ratio	v'	-	0,3	0,3	0,3
Poisson's ratio for unloading/reloading	v_{ur}	-	0,2	0,2	0,2
Shear strain for the 0.722 of the reduction of the shear modulus	$\gamma_{0.7}$	%	0,06	0,015	0,05
Power factor for the stress-level dependency of stiffness	m	-	0,6	0,6	0,6
Failure ratio	R_f	-	0,9	0,9	0,9
Angle of dilatancy	ψ	°	0	2	0
Coefficient of lateral earth pressure	k_0	-	0,700	0,470	0,642

3.3. Derivation of design seismic excitation

For the purpose of FE modeling of dynamic response of soil and structure the seismic excitation needs to be applied at the base of the finite domain of soil body. The strong ground motion which corresponds with the depth of the soil body`s base can be obtained by a deconvolution procedure.
Lets look at a 1D column of a soil profile which is presented as a SDOF system. The main idea is to explore the shear wave propagation through the soil layers and to generate a motion at a given depth in the soil profile. The latter is achieved by implementing the concept of transfer function, which is expressed by Equation 2.

$$H_{ij}(\mathrm{w}) = \left|\ddot{u}_i(w)\right| \Big/ \left|\ddot{u}_j(w)\right|, \qquad (2)$$

where: $\ddot{u}_i(w)$ – Fourier spectrum amplitude of the free surface motion, $\ddot{u}_j(w)$ – Fourier spectrum amplitude of the base motion.

Here in a conventional frequency-domain solution is used in order to deconvolve the surface ground motion to the base of the FE model (Poul and Zerva, 2018). The software ProShake 2.0 is used. The soil nonlinear behaviour is taken into account by applying the equivalent-linear constitutive model. To predict the corresponding shear modulus G and damping ratio ξ for each FE node i an iterative procedure is needed. The values of G_i and ξ_i, dependent on the maximum shear strain $\gamma_{max,i}$, are defined according to the reduction curves of (Vucetic & Dobri, 1991). As a result the design seismic excitations are obtained, which are applied to the base of the FE 2D model.
The retaining structure is examined for 6 earthquakes, selected to cover a large range of frequencies. The seismic impact is defined via accelerograms, scaled up to PGA = 1 m/s^2 – Figures 3, 5, 7, 9, 11 and 13.

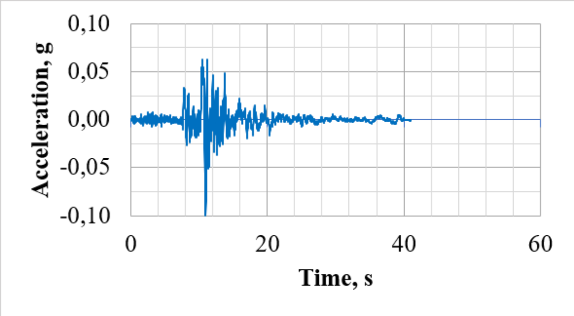

Figure 3. Accelerogram of the Loma Prieta EQ

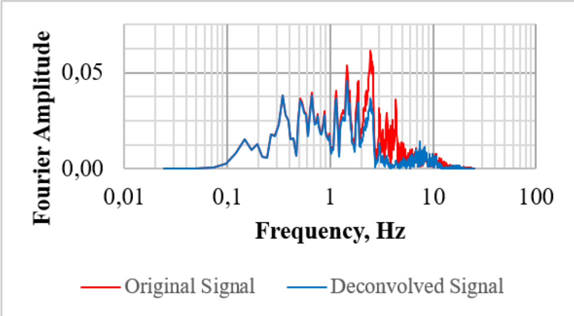

Figure 4. Fourier spectrum of the Loma Prieta EQ

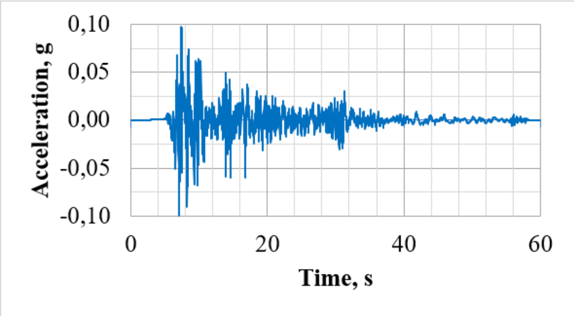

Figure 5. Accelerogram of the El Sentro EQ, 1940

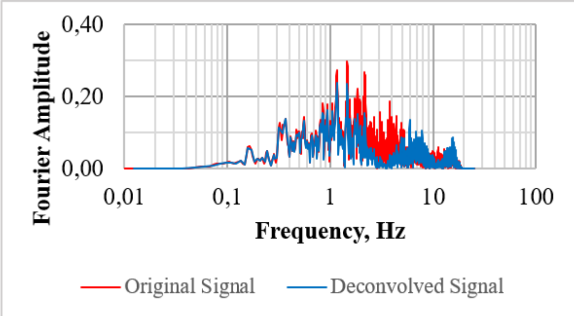

Figure 6. Fourier spectrum of the El Sentro EQ, 1940

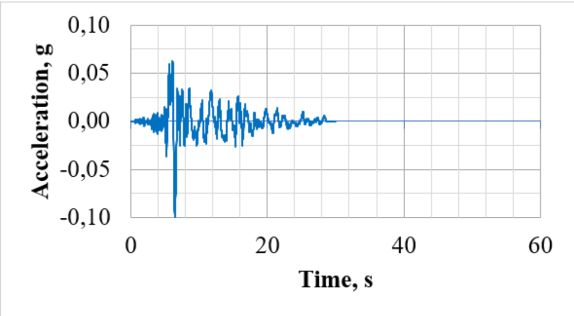

Figure 7. Accelerogram of the Cape EQ, 1992

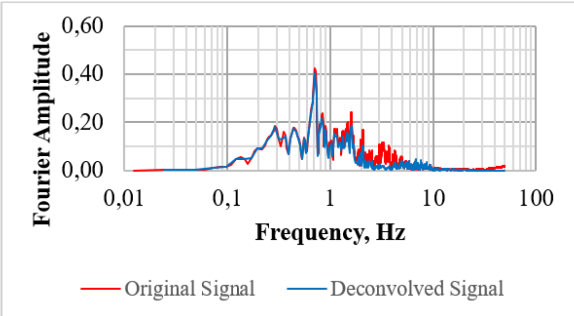

Figure 8. Fourier spectrum of the Cape EQ, 1992

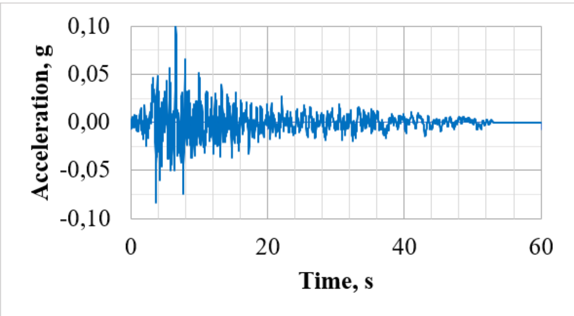

Figure 9. Accelerogram of the Taft EQ, 1952

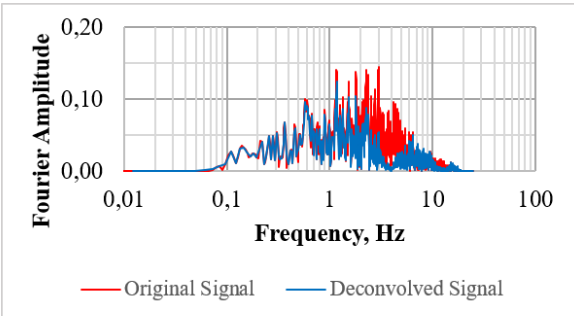

Figure 10. Fourier spectrum of the Taft EQ, 1952

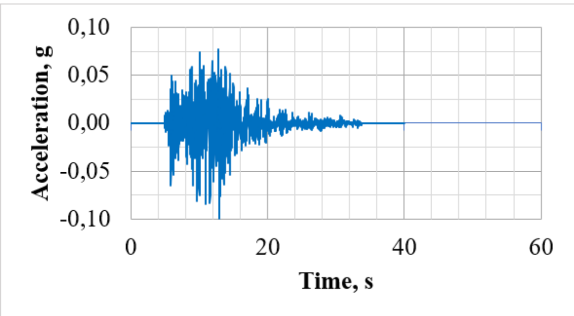

Figure 11. Accelerogram of the Northridge EQ, `94

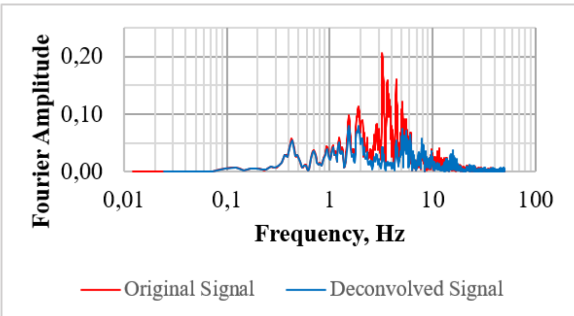

Figure 12. Fourier spectrum of the Northridge EQ,`94

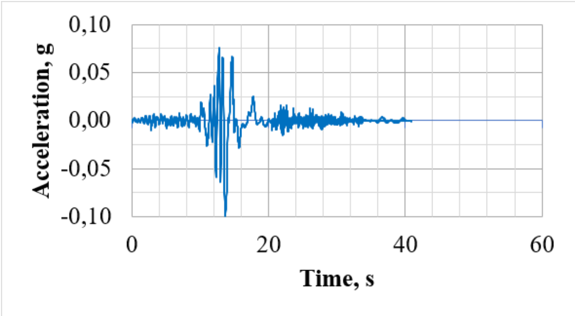

Figure 13. Accelerogram of the Loma Prieta EQ, record from Santa Cruz MTNS

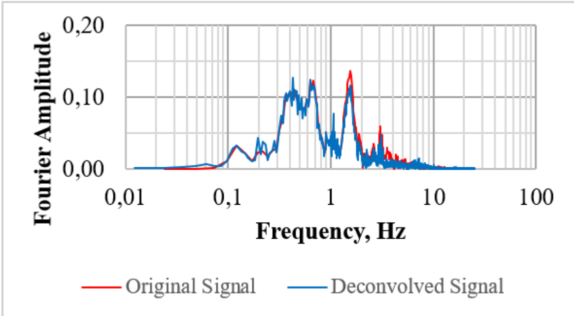

Figure 14. Fourier spectrum of the Loma Prieta EQ, record from Santa Cruz MTNS

In Figures 4, 6, 8, 10 and 12 a comparison between the original (surface) motions and the deconvolved ones is shown. It can be seen that the Fourier amplitude is increased when the seismic wave travels from the profile base to the terrain surface.

The design seismic impacts are rated by a set of peak and integral parameters. The characteristics are related to the deconvolved ground motions, which are used for the dynamic FE analysis. The ground motions` parameters are shown in Table 2.

Table 2. Parameters of the design seismic impacts

Eathquake	a_{max}	Predominant period, T_p	Mean period, T_m	Significant Duration, t_s	Arias Intensity, I_A
-	m/s^2	s	s	s	m/s
Loma Prieta EQ	1,0	0,40	0,86	24,02	0,054
El Sentro EQ	1,0	0,12	0,57	24,02	1,211
Cape Mendocino EQ	1,0	0,58	1,27	11,89	1,165
Taft, Kern County EQ	1,0	0,44	0,72	30,80	0,269
Northridge EQ	1,0	0,18	0,34	11,58	0,346
Loma Prieta EQ, Santa Cruz record	1,0	0,64	1,28	15,65	0,279

3.4. Frequency parameters of the foundation soil

The natural frequency of excitation is of essential importance for the effect of the ground motion on the retaining structure and the foundation soil. When the foundation soil`s natural period matches with the period of the earthquake, a state of resonance occurs. The resonance is associated with amplifying the dynamic load and its effects, which lead to failure of structure and soil.

The system soil-retaining wall, subjected to seismic load, is located in the city of Sofia, Bulgaria. The natural period is determined by Equation 3 (Kramer, 1996). The resulting value is T_s = 1,0 s.

$$T_S = \frac{4H}{V_S}, \tag{3}$$

where: H – thickness of the foundation soil [m]; V_s – shear wave velocity [m/s^2].

4. ANALYSIS OF THE RESULTS

Six dynamic analyses are performed with strong motions presented in Table 2. From the conducted solutions the diagrams of active and passive earth pressures are drawn. Here in Figure 16 are shown 3 typical diagrams of the examined seismic cases. The results for maximum earth pressures from analyses are listed in Table 3.

From the obtained results the envelope diagrams of bending moment M, shear force Q in the retaining wall and maximum horizontal displacement U_x, are reported. The values of the mentioned parameters, related to proper point of the wall, are placed in Table 3. In Figure 16 the general mode of M and Q diagrams are shown. The force`s distribution along the structure is typical for the adopted scheme.

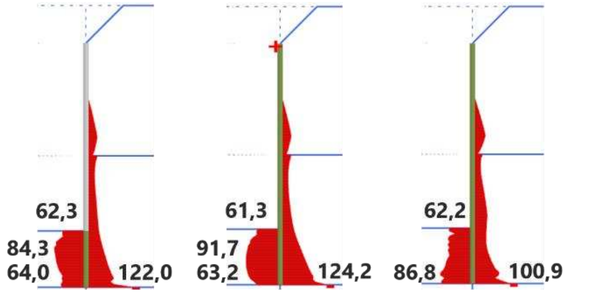

Figure 15. Typical modes of earth pressure diagrams Loma Prieta EQ, Northridge EQ and Loma Prieta EQ (SC)

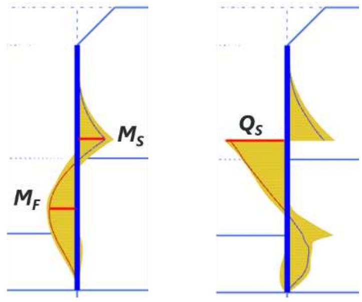

Figure 16. Typical modes of the envelope diagrams for bending moments and shear forces

Table 3. Results from the performed solutions

Earthquake	T_P	T_m	Bending moment, M_F	Bending moment, M_S	Shear force, Q_S	Lateral dis., U_x	Axial brace force, N	Earth pressure, p_a
-	s	s	kNm / m	kNm / m	kN / m	m	kN	kPa / m
Loma Prieta EQ	0,40	0,86	19,88	14,05	40,91	0,09	64,18	122,0
El Sentro EQ	0,12	0,57	20,24	13,99	42,48	0,05	68,29	120,7
Cape Mendocino EQ	0,58	1,27	26,26	16,41	49,94	0,12	79,15	125,0
Taft, Kern County EQ	0,44	0,72	20,70	13,81	41,18	0,08	64,39	122,2
Northridge EQ	0,18	0,34	18,46	13,14	38,55	0,03	61,05	124,2
Loma Prieta EQ, Santa Cruz record	0,64	1,28	28,63	17,78	50,81	0,13	83,00	100,9

Based on the strong ground motion parameters (Table 2) and the results presented in Table 3, several graphs are drawn. In Figure 17 to Figure 22 charts are shown, which illustrate the variation of bending moments (BM) M_F, shear forces (SF) Q_S and lateral displacement (LD) U_X versus predominant period T_P (graphic in red) and mean period T_m (graphic in blue).

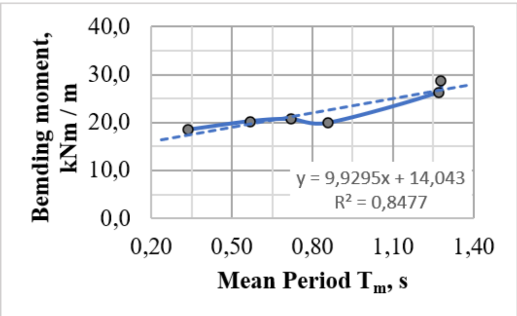

Figure 17. BM M_F versus mean period T_m

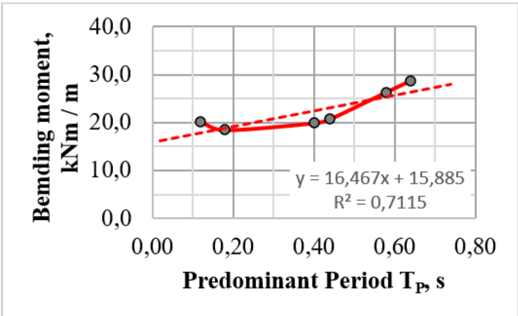

Figure 18. BM M_F versus predominant period T_P

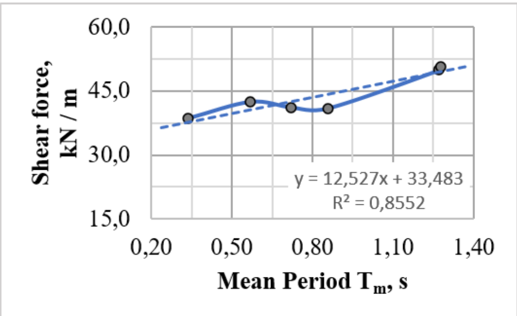

Figure 19. SF Q_F versus mean period T_m

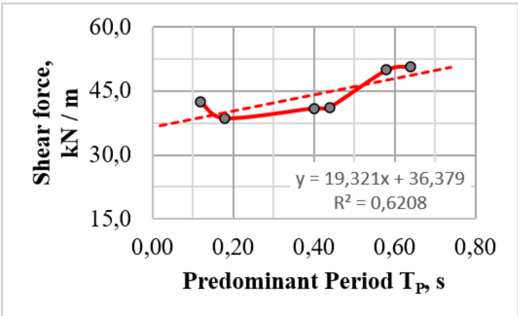

Figure 20. SF Q_F versus predominant period T_P

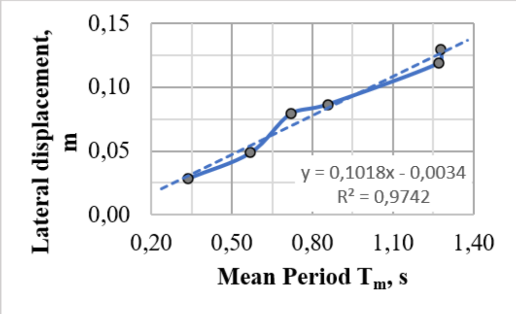

Figure 21. LD U_X versus mean period T_m

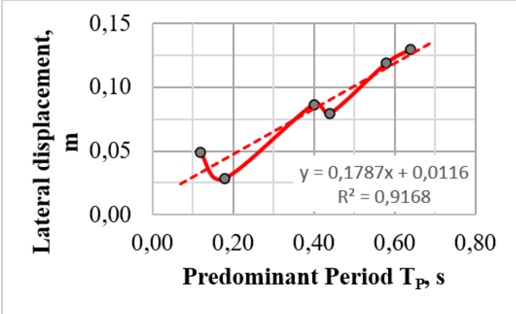

Figure 22. LD U_X versus predominant period T_P

A comparison is performed between the initial (target) seismic signal and the convolved one, obtained from the non-linear analysis in Plaxis 2D. The latter is reported from the free field of the soil body in the FE model. The comparison is made for one seismic motion – Taft EQ, but the results are valid for all the other motions. In Figure 23 and Figure 24 the time-histories and the Fourier spectrums are shown. Obvious distinctions are stated. The difference in the maximum acceleration amplitude is insignificant, but the frequency content is considerably different. The gap of mean period T_m for the pair of impacts amounts of almost 10%, but for the predominant period T_P it is more than 50%.
The quite different solution approaches and applied constitutive models for soils are pointed as the main reason for the observed discrepancies. Additional purposes are pointed as inconsistency of the boundary conditions between ProShake and Plaxis 2D, as well as inconformity of the modeled geometry (one-dimensional for ProShake and two-dimensioanl for Plaxis).

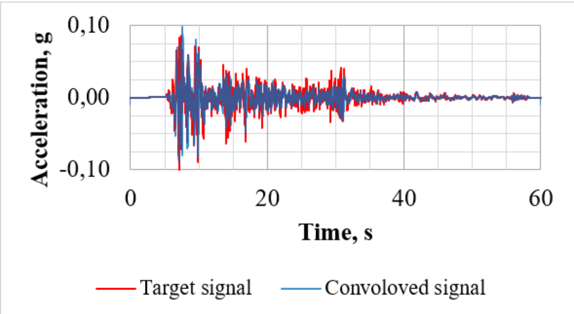

Figure 23. Comparison between target and convolved accelerograms of the Taft EQ, 1952

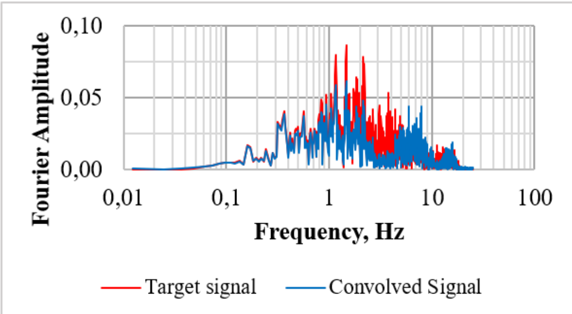

Figure 24. Comparison between target and convolved Fourier spectrums of the Taft EQ, 1952

Based on the comparative analysis the following conclusions can be drawn:
[1] The diagram of active earth pressure is lightly increasing as the bottom of the wall approaches – Figure 15. There is a leap in the diagram marked by the presence of a brace. The maximum value of active earth pressure is obtained for the Cape Mendocino EQ which is 20% higher than the minimum active earth pressure, accomplished by the Loma Prieta (Santa Cruz record) time history;
[2] The diagram of passive earth pressure receives various forms depending on the applied ground motion. For example – for the Loma Prieta EQ (Santa Cruz record) the passive pressure gradually increases as the bottom of the wall approaches. In contrary, for the case of Loma Prieta EQ the passive pressure decreases with depth. In similarity with the active pressure, the highest value of passive pressure is obtained from the Cape Mendocino EQ;
[3] According to the distributions on Figure 17 – Figure 22, a general trend of increasing in forces and displacements as the natural period of foundation soil T_S approaches, is formed;
[4] As the presented diagrams evidence (Figure 17 – Figure 22), the forces and displacements\` distribution for the mean period T_m is more satisfactory than the one for the predominant period T_p. The difference in values of the coefficient of correlation amounts of 16% for the BM and 27% for the SF. This leads to the conclusion that the seismic response of structure depends mainly and more accurately on the mean period T_m;
[5] The Cape Mendochino EQ and the Loma Prieta EQ (Santa Cruz record) are the most unfavourable ground motions, that is proved by the highest values for inertial forces, lateral displacement and earth

pressure. This is because the seismic loadings have a mean period T_m = 1,2 – 1,3 s, which is the closest value to the natural period of soil T_P = 1s. In such a case the foundation soil falls into a state close to the resonance. Then an amplification of the impact and the subsequent reaction of the structure take place, which is the purpose for the most adverse response;
[6] For the Cape Mendochino EQ and the Loma Prieta EQ (Santa Cruz record) similar stress values are accomplished. Taking into account for the frequency parameters, the latter statement is fully understandable. The stresses for the Loma Prieta EQ are little higher. The difference in stresses is barely 10% for the BM and 15% for the SF. This is explained with the higher significant duration of the Loma Prieta EQ, which calls forth more reversal cycles and increased degradation of shear stiffness of soil;

5. CONCLUSIONS

In the present study a set of solutions are carried out in order to examine the seismic response of an embedded retaining wall. The soil-structure interaction is simulated by a FE plane strain model. The Plaxis 2D software is used. The hysteresis behaviour of soils due to cyclic dynamic loading is taken into account by applying the HSsmall constitutive model.
The seismic impact is determined by accelerograms. Six accelerograms of real earthquake events are used. The records are previously subjected to a deconvolution procedure in order to obtain the input signal to the base of the FE model. The deconvolution is performed by the ProShake software for 1D wave propagation analysis.
Based on the analysis and comparisons of the obtained results conclusions are drawn. It is shown that the seismic response of the wall depends mostly on the frequency characteristics of the foundation soil and the ground motion – in particular the natural period of soil T_s and the mean period of the earthquake impact T_m.
It is proved that the deconvolution procedure conducted by the ProShake software is not the most appropriate method when there is a non-linear analysis subsequently carried out. Some discrepancies between the convolved time-history signal from the non-linear analysis and the initial (target) time history will surely occur. They are presented mostly by differences in the amplitude and frequency content of the ground motion. That is why a deconvolution of seismic waves from time-domain non-linear analysis is recommended.

REFERENCES

Kerenchev, N. 2015. Analysis of seismic slope stability and deformations PhD Thesis. *University of Architecture Civil Engineering and Geodesy*, Sofia, Bulgaria

Kerenchev, N., Milev, N. 2019. Assessment of the dynamic soil properties for the FEM model of the Liuliakovitsa Tailings Dam. *Proc. of the 8th Conference Geotechnics in Civil Engineering*, Vrnjačka Banja, Serbia

Kramer, S. 1996. Geotechnical Earthquake Engineering. *Prentice Hall, Upper Saddle River, New Jersey 07458*

Kuhlmeyer, R.L., Lysmer, J. 1973. Finite element method accuracy for wave propagation problems. *Journal of the soil mechanics and foundation division*, Vol. 99, pp. 421-427

Poul, M. K., Zerva, A. 2018. Efficient time-domain deconvolution of seismic ground motions using the equivalent-linear method for soil-structure interaction analyses.

Schanz T., Vermeer P.A., Bonnier P.G. 1999. The hardening soil model: Formulation and verification. *Beyond 2000 in Computational Geotechnics - 10 Years of PLAXIS*, Balkema, Rotterdam

Vucetic, M., Dorby, R.. 1991. Effect of soil plasticity on cyclic responses. *Journal of geotechnical engineering*, ASCE 117(GT1), pp. 89–107